Published in final edited form as:
Circ Res. 2009 February 27; 104(4): 488–495. doi:10.1161/CIRCRESAHA.108.185777.

TLR4 and TLR5 induce distinct types of vasculitis

Jiusheng Deng[*], **Wei Ma-Krupa**[*], **Andrew T. Gewirtz**, **Brian R. Younge**, **Jörg J. Goronzy**, and **Cornelia M. Weyand**
The Lowance Center for Human Immunology and Rheumatology, Emory University School of Medicine, 101 Woodruff Circle, Atlanta, GA 30322

Abstract

Large vessel vasculitides, such as Takayasu arteritis and giant cell arteritis (GCA), affect vital arteries and cause clinical complications by either luminal occlusion or vessel wall destruction. Inflammatory infiltrates, often with granulomatous arrangements, are distributed as a panarteritis throughout all of the artery's wall layers or cluster in the adventitia as a perivasculitis. Factors determining the architecture and compartmentalization of vasculitis are unknown. Human macrovessels are populated by indigenous dendritic cells (DC) positioned in the adventitia. Herein, we report that these vascular DC sense bacterial pathogens and regulate the patterning of the emerging arteritis. In human temporal artery-SCID chimeras, lipopolysaccharides stimulating Toll-like receptor (TLR) 4 and flagellin stimulating TLR5 trigger vascular DC and induce T-cell recruitment and activation. However, the architecture of the evolving inflammation is ligand specific; TLR4 ligands cause transmural panarteritis and TLR5 ligands promote adventitial perivasculitis. Underlying mechanisms involve selective recruitment of functional T cell subsets. Specifically, TLR4-mediated DC stimulation markedly enhances production of the chemokine CCL20, biasing recruitment towards CCL20-responsive CCR6+ T cells. In adoptive transfer experiments,$CCR6^+$ T cells produce an arteritis pattern with media-invasive T cells damaging vascular smooth muscle cells. Also, $CCR6^+$ T cells dominate the vasculitic infiltrates in patients with panarteritic GCA. Thus, depending on the original danger signal, vascular DC edit the emerging immune response by differentially recruiting specialized T effector cells and direct the disease process toward distinct types of vasculitis.

Keywords

T cell; Toll-like receptor; inflammation; vascular inflammation

Introduction

Inflammatory vasculopathies targeting human medium and large arteries are debilitating and life-threatening diseases as they damage vital arteries and cause aortic aneurysms, cerebral ischemia, and aortic arch syndrome.[1] Takayasu arteritis (TA) typically manifests in the aorta and its primary branches of young women, and giant cell arteritis (GCA) affects the aorta and its more distal branches in older individuals. The underlying process is a granulomatous inflammation accumulating within the vessel wall with typical granulomas and multinucleated giant cells or a diffuse lympho-monocytic infiltrate.[2] Inflammatory cells access the artery

Address Correspondence to: Cornelia M., Weyand, MD, PhD, Lowance Center for Human Immunology, WMRB #1003, 101 Woodruff, Circle, Atlanta, GA 30322; telephone (404) 727-7310; fax: (404) 727-7371; cweyand@emory.edu.
[*]These authors contributed equally to this work.

Subject codes: [97] Other Vascular Biology, [130] Animal models of human disease

Disclosures
None.

through adventitial vasa vasorum, not the macrolumen.[3] In a patient subset, the arteritis histomorphology is that of perivasculitis, also called vasa vasoritis, with smaller arterial branches in the adventitia as the primary target.[4–6] How immune responses are compartmentalized to cause adventitial arteritis or transmural arteritis is not understood. Whether inflammatory effectors causing either of these disease architectures are identical or distinct is unknown. In both TA and GCA, CD4 T cells are the dominant lymphocyte population, accompanied by few CD8 T cells and rare NK cells and γδ-T cells.[7] In GCA arteries, local immune responses are strongly biased toward IFN-γ production, with IL-4 essentially absent.[3] Mechanisms through which the vessel wall edits the cytokine milieu are unidentified; possibilities include differential priming of T effectors or selective recruitment of committed effector populations. In GCA-affected arteries T-cell populations are selected for specificity, with identical clonotypes isolated from anatomically distinct arteries.[8, 9] Priming of these clonotypes may occur in the lymph node. Alternatively, the local tissue site dictates which T cells are primed or recruited. In macrophages, functional commitment and topographic location in the vessel wall are closely correlated, emphasizing the potential impact of the microenvironment.[10]

Organs exposed to the outside world, such as the skin and the mucosal surfaces, have tissue-specific innate immune systems[11] with dendritic cells (DC) functioning as potent immunosensors screening for local danger signals. Surprisingly, human macrovessels share with these tissues pathogen-sensing ability [12]. Equipped with DC populations positioned at the media-adventitia border, medium and large arteries recognize pathogen-derived motifs.[13, 14] DC are the principal antigen-presenting cells (APC) in ongoing GCA.[15] In bioengineered human macrovessels, wall-embedded DC—but not monocytes and macrophages—have APC function and trigger intramural adaptive immune responses.[16]

Human macrovessels express a broad spectrum of TLR, overall biased towards receptors recognizing bacterial products [12]. Remarkably, each vascular territory has a unique TLR profile suggesting specialization in immunosensing functions. It is unknown whether recognition of different TLR ligands induces similar or distinct biologic effects. The current study has explored this question in human temporal arteries, the preferred target of GCA, and has examined whether bacterial products binding to different TLR induce distinct types of vessel wall inflammation. Dependent on the initial danger signal, vascular DC adapted their chemokine profile and selectively recruited specialized T-cell effectors. Whereas TLR4 agonists induced CCL20 favoring the recruitment of media-invasive $CCR6^+$ T cells, TLR5 ligands facilitated adventitial immune responses. Wall infiltration by $CCR6^+$ cells resulted in vascular smooth muscle cells (VSMC) injury, a typical component of vasculitis. In GCA patients, $CCR6^+$ T cells dominate the wall infiltrate. Separating patients with large-vessel vasculitis into those with transmural panarteritis and those with vasa vasoritis will allow searching for selective disease instigators.

Materials and Methods

Human temporal arteries, lymph nodes, and skin

Thirty-eight temporal artery specimens were collected by diagnostic temporal artery biopsy or harvested at postmortem examination. Normal arteries derived from patients with no clinical evidence for polymyalgia rheumatica or any other vasculitic syndrome, lacked inflammatory infiltrates, and had no changes indicating atherosclerosis. Vessels were cut into 5 mm pieces and used immediately for culture *in vitro* or engrafted into immunodeficient mice. For RNA extraction, arteries were immediately shock frozen and for immunohistochemical staining, specimens were embedded in OCT compound (Sikura Fine-Tek, Torrance, CA). Human lymph nodes and skin were collected from surgical waste tissues and processed immediately after

removal. All protocols were approved by the Institutional Review Boards, and appropriate consent was obtained.

Reagents

LPS (*Escherichia coli, 0127:B8*), Poly (I:C), LTA, and CpG were purchased from Sigma-Aldrich (St. Louis, MO). Flagellin was purified as described previously [17] or obtained from InvivoGen (San, Diego, CA).

Isolation of cells

Human peripheral blood was obtained from healthy donors and mononuclear cells (PBMC) were isolated by Ficoll-Paque (Mediatech, Manassas, VA). $CD14^+$ cells were purified with anti-human CD14 MicroBeads using the AutoMACS system (Miltenyi Biotec, Auburn, CA). Monocyte-derived DC were generated from $CD14^+$ precursors at 37°C for 5–6 days in RPMI 1640, supplemented with 1,600 U/ml of recombinant human GM-CSF, and 1,000 U/ml of recombinant human IL-4. CD4 T cells were purified with anti-human CD4 MicroBeads (Miltenyi Biotec) for T-cell migration assays or for T-cell adoptive transfers. $CCR6^+$ cells were depleted from PBMC with PE-conjugated mouse anti-human CCR6 antibodies (BD Pharmingen) and anti-PE microbeads.

In vitro organ culture

Intact human lymph nodes, skin, or temporal arteries were cultured in RPMI 1640 (10% FCS) in 48-well flat-bottom plates and stimulated with different TLR ligands: LTA (500μg/ml), Poly (I:C) (100μg/ml), LPS (3μg/ml), flagellin (3μg/ml), or CpG (50μg/ml) for 14 h at 37°C. Tissues were then harvested and used for RNA isolation. For kinetic CD83 gene induction assays, tissues were stimulated with LPS (3μg/ml) or flagellin (3μg/ml) for 12, 24, or 48 h. In selected experiments, temporal arteries were cultured with 1×10^6 human CD4 T cells for 3 days after stimulation with TLR ligands.

Quantitative Real-Time PCR

RNA transcripts were quantified by real-time PCR as described and adjusted to 2×10^5 copies of the housekeeping gene β-actin.[15] Specific PCR primers are listed in Online Table I.

Immunostaining of tissue sections

OCT-embedded arteries were sectioned at 7μm intervals and immunostained as described[15] using the following primary antibodies: mouse anti-human CD3 (1:200, Dako, Carpinteria, CA), mouse anti-human TLR4 (1:100; Biotechnology, Santa Cruz, CA), mouse anti-human TLR5 (1:100; Imgenex, San Diego, CA), or mouse anti-human CCR6 (1:100; R&D Systems, Minneapolis, MN). Isotype-matched primary antibodies served as control. Antibody binding was visualized with biotin-conjugated goat anti-mouse IgG (BD PharMingen, San Diego, CA). Tissue sections were stained with propidium iodine (PI) (Sigma) and examined by fluorescence microscopy. Sections from paraffin-embedded temporal arteries were de-waxed before being treated with mouse anti-human CCR6 antibody at 4°C overnight. To quantify tissue-invasive capability, T cells were stained with anti-CD3 antibodies and their distance to the tissue surface was measured utilizing Image J1.36b software (NIH, USA).

Human Temporal Artery-SCID Mouse Chimeras

Human temporal artery-SCID mouse chimeras were generated by subcutaneous implantation of temporal artery sections into NOD.CB17 Prkdc (SCID) mice (Jackson Labs, Harbor, ME) as previously described.[15] Three mice implanted with temporal artery tissues from the same donor were assigned to two treatment arms and a control arm. On day 7 after implantation,

mice were injected with LPS (3μg/mouse), flagellin (3μg/mouse), or PBS. On day 8, PBMC or PBMC depleted of $CCR6^+$ T cells (3×10^7 cells/mouse) or CD4 T cells (10^7 cells/mouse) were adoptively transferred into the chimeras by i.v. injection. On day 15, arterial grafts were harvested for RNA extraction or embedded into OCT compound for immunostaining. The protocol was approved by the Emory University Institutional Animal Care and Use Committee.

Statistical Data Analysis

Results were analyzed using the two-sided Student's t test. Data are shown as mean ± standard error (SEM).

Results

TLR4 and TLR5 ligands activate resident DC in temporal arteries

To explore whether human arteries respond to different pathogen-associated patterns with distinct biologic outcomes, human temporal arteries were stimulated with a panel of TLR ligands (Fig. 1A). Based on previous studies establishing TLR expression patterns in human macrovessels[12] LTA (TLR2/6 ligand), Poly (I:C) (TLR3 ligand), LPS (TLR4 ligand), flagellin (TLR5 ligand), and CpG (TLR9 ligand) were chosen as stimulatory agonists. Response patterns were quantified by the induction of CD83 transcripts, a sensitive measure of DC activation. In pilot experiments, optimal stimulatory concentrations for each ligand were determined. Response patterns of temporal arteries were compared to that of two DC-rich tissues, human lymph nodes and skin (Fig. 1A and Online Table II). LPS and flagellin emerged as the two strongest stimulators of arterial tissues with a 16-fold and 30-fold upregulation of CD83 transcripts, respectively (Fig. 1A). Transcript induction translated into surface expression of CD83 protein (Fig. 1C). LPS-mediated activation was maximal after 12h and rapidly declined at 24 and 48h. TLR5 ligation resulted in prolonged DC activation with CD83 transcripts at a plateau between 12 and 24h (Online Fig. I). TLR3 and TLR9 ligands barely elicited a temporal artery response; both were efficiently detected by lymph nodes (Online Table II). The three tissues each displayed a unique TLR response profile. Skin was explicitly sensitive to TLR4 ligands, unresponsive to TLR5 agonists, reactive to TLR3, and minimally affected by CpG. Lymph nodes sensed each of the pathogen-derived patterns; however, CD83 induction varied widely among different agonists. Notably, the three tissues appeared to recognize each TLR ligand with differential efficiency. These experiments established selectivity in the TLR responsiveness of human organs and indicated that temporal arteries were particularly sensitive to TLR4 and TLR5 ligands.

As arterial walls are complex structures, we examined which cells in temporal arteries carried TLR4 and TLR5 receptors. Tissue extracts contained high and comparable transcript levels for the DC markers CD11c and CD209 (DC-SIGN), but lacked the macrophage marker CD11b (Fig. 1B). TLR4 and TLR5 transcripts were abundant and present in similar concentrations. Endothelial cells and VSMC in vitro have been described as positive for TLR4 but immunohistochemical stains of normal arteries localized TLR4 proteins on spindly cells at the media-adventitia border (Fig. 1D, F). von Willebrand Factor (vWF)-positive macroluminal endothelial cells had minimal TLR4 reactivity and the micro-endothelial cells of the vasa vasorum were consistently negative. Staining of serial tissue sections with anti-TLR4 and anti-CD209 or anti-TLR5 and anti-CD209 provided unequivocal evidence that the TLR-expressing cells were DC (Fig. 1F and 1G inserts).

TLR4 and TLR5 ligands induce differential patterns of adaptive immune responses in the vessel wall

To determine whether the mode of activation affected evolving immune responses in the vascular wall, the effects of TLR4 and TLR5 ligands on T-cell immunity were compared.

Temporal arteries from the same donor were engrafted into multiple SCID mice, and T-cell responses were probed by adoptive transfer of allogeneic CD4 T cells. LPS or flagellin pretreatment resulted in prompt and comparable T-cell recruitment and in situ activation (Fig. 2A and Online Fig. II). Similarly, stimulation of human temporal arteries in organ culture demonstrated that both TLR4 and TLR5 agonists initiated adaptive immune responses and facilitated recruitment of human T cells into the vessel wall. In the chimera system, concentrations of IFN-γ transcripts indicated similar efficiency of TLR4 and TLR5-sensing DC in stimulating T cells (Online Fig. II). However, spatial analysis of tissue-infiltrating lymphocytes in the arteries revealed fundamental differences in the immune responses initiated by TLR4 or TLR5 ligands. Immunohistochemistry demonstrated tissue-invading T cells in the media of LPS-stimulated vessels whereas the smooth muscle cell layer remained essentially T-cell free in TLR5-triggered arteries (Fig. 2B). Conversely, $CD3^+$ T cells accumulated in the adventitia of arteries exposed to flagellin (Fig. 2 C, F). In essence, tissue inflammation patterns were closely correlated with the pathogen-derived motif initially recognized by the vascular DC. LPS, but not flagellin, endowed vascular DC with the ability to recruit and/or instruct T cells to generate wall-penetrating infiltrates. Conversely, flagellin produced T-cell recruitment and activation patterns resembling perivasculitis.

TLR4 ligation selectively upregulates CCL20 expression and induces $CCR6^+$ CD4 T-cell recruitment in vitro and in vivo

As site-specific T-cell accumulation was determined by the initial mode of DC activation, we explored how TLR4 and TLR5 ligands differentially affected DC function. Utilizing a gene array tailored for activated DC, we compared a series of 58 gene transcripts following LPS or flagellin stimulation in vitro. In 4 independent experiments, the induction of 47 genes, including DC markers CD83 and CD86, was very similar under both activation conditions. A set of 11 genes, including the chemokine CCL20, was differentially induced (Fig. 3A). Compared to unstimulated DC, LPS upregulated CCL20 expression 6.5 fold whereas flagellin enhanced CCL20 transcripts only by 2.8 fold. Quantification of CCL20 transcripts by real-time PCR in LPS- or flagellin-treated DC corroborated the gene array data. (Fig. 3B). CCL20 exclusively binds to CCR6, a receptor expressed on a specialized T-effector cell subset. To prove functional relevance, chemoattraction of CD4 T-cell subsets was evaluated in migration assays using modified Boyden chambers. In vitro-generated DC placed in the lower chamber remained untreated or were stimulated with LPS or flagellin. T cells positioned in the upper chamber were allowed to migrate toward the chemokine-producing DC. After 2 h, T cells attracted by untreated DC included only 10% of $CCR6^+$ CD4 T cells. Flagellin-triggering of the DC did not affect the representation of $CCR6^+$ CD4 T cells. However, after LPS stimulation, DC selectively attracted $CCR6^+$ CD4 T cells enriching them to 32% (Fig. 3C).

To determine whether LPS treatment in vivo was associated with preferential recruitment of $CCR6^+$ T cells and infiltration of T cells into the deep wall layers, temporal artery-SCID chimeras were injected with LPS or flagellin before human CD4 T cells were infused. Artery explants were analyzed for CCL20 and CCR6 transcripts; tissue sections were examined for $CCR6^+$ T cells invading into the wall layers. CCL20 and CCR6 expressions were significantly higher in the grafts of LPS-treated chimeras, whereas flagellin failed to upregulate CCL20 and enhanced CCR6 transcripts slightly (Online Fig. III and Fig. 4). Numeric analysis of $CCR6^+$ and $CCR6^-$ T cells in the medial and the adventitial compartment clearly demonstrated the preference of $CCR6^+$ cells for the medial layer. Adventitial infiltrates contained more $CCR6^-$ T cells (Fig. 4B). Thus, positioning and retention of T cells in distinct regions of the vessel is closely correlated with T-cell phenotype and function.

CCR6$^+$ T cells in the vasculitic infiltrates of GCA

To test whether CCR6$^+$ T cells populate the panarteritic infiltrates in GCA, we analyzed inflamed temporal arteries from GCA patients and stained circumferential sections with CCR6-specific antibodies. CCR6 receptors were expressed on the majority of mononuclear cells but not giant cells and histiocytes within the inflammatory infiltrates (Fig. 4F). Most lymphocytes infiltrating the lumen-occlusive intima stained positive. Adventitial infiltrates included a low frequency of CCR6$^+$ cells (Fig. 4E). CCR6$^+$ cells accumulated at the intima-media junction surrounding giant cells and the fragmented elastic lamina (Fig. 4F). Overall, the immunohistochemical analysis confirmed strong CCR6$^+$ T-cell enrichment in the vasculitic infiltrates and the relevance of the CCL20-CCR6 axis in large-vessel vasculitis.

CCR6 blockade abrogates CD4 T-cell invasion and prevents VSMC damage

TLR4-mediated CCL20 induction and CCR6$^+$ T-cell accumulation in the GCA lesions suggested a unique role of CCR6$^+$ T cells in transmural arteritis. Human arteries were engrafted into SCID mice; chimeras were injected with LPS or sham treated, and CD4 T cells were adoptively transferred 24 h later. These CD4 T cells were co-administered with anti-human CCR6 antibodies or isotype control antibodies. TLR4 ligation promoted accumulation of vessel wall infiltrates (Fig. 5A). Disrupting the CCL20-CCR6 axis by co-administering anti-CCR6 abrogated the media-invasive phenotype of the developing vasculitis. In chimeras injected with CD4 T cells precoated with anti-CCR6 antibodies, T-cell infiltrates were restricted to the adventitia (Fig. 5B, D). To quantify media invasion, the migration depths of individual T cells were measured by digital analysis of tissue sections stained for the T-cell marker CD3 (Fig. 5D). Without LPS, few T cells were recruited to the arteries, none migrating deeper than 50 μm. After TLR4 ligation, CD4 T cells invaded deeply into the wall, on average 300 μm, with the most advanced T cells passing almost 1000 μm. After antibody-mediated CCR6 blockade, the migration capacity of activated T cells was markedly impaired; CD4 T cells were retained in the adventitia, only a few progressed into the smooth muscle cell layer.

To explore whether invading T cells caused VSMC damage, we measured the transcriptional activity for smoothelin, a molecule typically produced by healthy contractile smooth muscle cells. Loss of smoothelin-specific transcripts is a typical finding for arteries affected by GCA (Fig. 5E). Adoptive transfer of anti-CCR6-coated CD4 T cells protected smoothelin production, indicating that CCR6 blockade shields the tissue from inflammatory damage (Fig. 5F).

CCR6-positive T cells possess tissue-invasive capabilities in vascular inflammation

To confirm that a specialized CCR6$^+$ T-cell subset is responsible for causing panarteritis, we compared the vascular inflammation patterns mediated by PBMC containing the CCR6$^+$ subpopulation or depleted of CCR6$^+$ cells. Normal human arteries were engrafted, and chimeras were LPS conditioned or sham treated. PBMC for adoptive transfer were left un-separated or depleted of CCR6-expressing cells. Recruited cells assumed a characteristic distribution (Fig. 6). T-cell recruitment into the vessel wall occurred only if un-separated PBMC were transferred (Fig. 6A). CCR6$^+$ cell depletion essentially abrogated vascular infiltrate formation. Enumeration of media-residing cells demonstrated minimal infiltrates in the grafts of sham-treated chimeras and in grafts of chimeras injected with CCR6-depleted cell preparations. Dense cell infiltrates accumulated among the medial VSMC if un-separated PBMC were transferred (Fig. 6B). Direct visualization of tissue-invasive cells demonstrated marked differences in the architecture of vasculitic infiltrates. Without LPS pretreatment, cells failed to enter the smooth muscle cell layer (Fig. 6C). Crowded cellular infiltrates accumulated between the smooth muscle cell lamellae if vascular DC were activated through TLR4 ligation and the adoptive transfers provided CCR6$^+$ cells (Fig. 6D). Depletion of CCR6$^+$ cells prevented

infiltration of adoptively transferred cells into the media (Fig. 6E). These experiments supported a selective role of $CCR6^+$ T cells in causing panarteritis.

Discussion

Human medium and large arteries are populated by vascular DC that sense pathogens and induce adaptive and vasculitic immune responses in the vessel wall.[12] In the atherosclerotic plaque, wall-residing DC sustain and amplify inflammation.[18] Herein we show that the role of vascular DC extends beyond enhancing immunity but that the activation mode determines the architecture of the immune response emerging in the vessel wall. TLR4 ligation leads to transmural panarteritis, with CD4 T cells invading into the proximal wall layers and injuring VSMC. Conversely, TLR5 triggering mediates the assembly of a perivasculitis with T cells accumulating in the adventitia. Our mechanistic studies show that TLR4-stimulated DC preferentially produce CCL20, resulting in the recruitment and activation of a specialized $CCR6^+$ T-cell subset. T-cell infiltrates in the medial smooth muscle cell layer are highly enriched for $CCR6^+$ cells which may find optimal survival conditions in this microenvironment. Thus, vessel-wall embedded DC not only initiate adaptive immune responses; they shape the inflammation's architecture, and different bacterial pathogens induce distinct vasculitis types. Categorizing patients with large-vessel vasculitis according to the inflammation's patterning may provide an important clue in the search for causative agents.

Human macrovessels display a broad spectrum of pattern-recognition receptors, but it is not known whether biologic outcomes of recognizing "danger signals" is uniform or is specific for the stimulator. Human temporal arteries responded to a series of pathogen-derived motifs with a tissue-specific response, distinct from that of the skin and the lymph node. Intact arteries appeared to specialize in detecting bacterial products binding TLR 4 or 5, yet the biologic consequences were ligand-specific. TLR4 ligation resulted in T-cell recruitment into the media, recapitulating the positioning of panarteritic T cells. Flagellin was highly effective in instructing wall-residing DC to induce IFN-γ in T cells. However, responsive T cells were functionally distinct from those attracted to LPS-sensitized DC. They failed to display tissue-invasive character, clustered in the adventitia, and produced a perivasculitis. Immunohistochemical studies assigned TLR5 expression exclusively to cells expressing the DC marker CD209. TLR4 has been reported to also be expressed on endothelial cells and VSMC [19, 20] in vitro and under inflammatory vessel wall remodeling conditions. In healthy human arteries, the expression of TLR4 is literally limited to wall-integrated $CD209^+$ cells (Fig. 1).[12]

The TLR9 nonresponsiveness of temporal arteries (Fig. 1, Online Table II) is in line with the lack of plasmacytoid DC in normal arterial walls whereas that DC subtype is critically involved in amplifying inflammation in the atherosclerotic plaque [18].

Current data implicate $CCR6^+$ T cells as particularly relevant in mediating vasculitis, at least in GCA. Several lines of evidence link $CCR6^+$ CD4 T cells to the panarteritic pattern of vasculitis. $CCR6^+$ cells populate the inflammatory infiltrates in GCA-affected arteries (Fig. 4). CCR6 antibody blockade abrogates media-penetrating infiltrate formation, and $CCR6^+$ T-cell depletion disrupts transmural infiltrates and restricts T cells to the adventitia (Fig. 5, Fig 6).

Here we propose that $CCR6^+$ T cells are a potential target for therapeutic interventions in large-vessel vasculitis. So far the CCL20-CCR6 axis has been implicated ensuring protective immune responses.[21] CCL20 regulates turnover and positioning of $CCR6^+$ immature DC in peripheral tissues. In GCA lesions, DC are greatly enriched and participate in forming the granulomas. Possibly, CCL20 production by wall-residing DC facilitates further influx of DC,

enhancing their role in granuloma stabilization. Staining of GCA arteries with anti-human CCL20 antibodies ruled out its expression by the medial layer of smooth muscle cells or endothelial cells (data not shown). CCL20-CCR6 interactions shape intestinal immunity and lympho-organogenesis.[22] Produced by intestinal epithelial cells, CCL20 orchestrates B-cell recruitment and the formation of lymphoid follicles in the gut. Besides B cells and immature DC, multiple T-cell subsets express CCR6. CCL20 directs activated T cells into the skin during contact hypersensitivity.[23] Asthmatic patients preferentially mobilize $CCR6^+$ T cells during allergic responses.[24] Recently, CCR6 has been identified on multiple Th17 cell subsets as well as other regulatory T-cell subsets, specifically $Foxp3^+$ T cells.[25] CCR6 appears on Tr1 cells and on $CD8^+$ effector memory T cells. CD8 T cells as well as $Foxp3^+$ cells are explicitly infrequent in GCA lesions (data not shown), suggesting an unopposed pro-inflammatory role for $CCR6^+$ CD4 T cells in this vasculitis. Blockade of CCR6 disrupted tissue damage in the artery; precisely, it restored production of smoothelin, a VSMC molecule linked to contractility. This observation identifies VSMC as a direct target of T cell-mediated wall injury.

Corticosteroids, commonly used to treat GCA and TA, target the pro-inflammatory transcription factor NF-κB.[26] CCL20 gene transcription and production are controlled by NF-κB and sensitive to ERK1/2 and p38/MAPK inhibitors.[27] Thus, current treatment may actually target the CCL20-CCR6 axis. With the devastating side effects of steroid therapy, a more sophisticated way of paralyzing $CCR6^+$ T cells could revolutionize the therapy of large-vessel vasculitis.

As yet, the causative agents initiating GCA remain elusive. Data presented here suggest that innate immune reactions, shaped by vascular DC, are not only inductive for arteritis but also determine the architecture and organization of the pathogenic response. The correlation between the mode of DC activation and the vasculitis pattern may provide useful clues in the identification of disease instigators. Based on biopsy findings, patients should be categorized into those with panarteritis and periarteritis as a means of defining more homogenous subsets for pathogenic and therapeutic studies.

Supplementary Material

Refer to Web version on PubMed Central for supplementary material.

Acknowledgment

The authors thank Tamela Yeargin for manuscript editing.

Sources of Funding

This work was supported by grants from the National Institutes of Health (RO1 EY11916, RO1 AI44142, RO1 AR42527, RO1 AG15043, RO1 AR41974) and the Dana Foundation.

References

1. Weyand CM, Goronzy JJ. Medium- and large-vessel vasculitis. N Engl J Med 2003;349:160–169. [PubMed: 12853590]
2. Gravanis MB. Giant cell arteritis and Takayasu aortitis: morphologic, pathogenetic and etiologic factors. Int J Cardiol 2000;75:S21–S33. [PubMed: 10980333]discussion S35–26.
3. Wagner AD, Bjornsson J, Bartley GB, Goronzy JJ, Weyand CM. Interferon-gamma-producing T cells in giant cell vasculitis represent a minority of tissue-infiltrating cells and are located distant from the site of pathology. Am J Pathol 1996;148:1925–1933. [PubMed: 8669478]
4. Nordborg C, Larsson K, Nordborg E. Stereological study of neovascularization in temporal arteritis. J Rheumatol 2006;33:2020–2025. [PubMed: 16924688]

5. Numano F. Vasa vasoritis, vasculitis and atherosclerosis. Int J Cardiol 2000;75:S1–S8. [PubMed: 10980330]discussion S17–19.
6. Chatelain D, Duhaut P, Loire R, Bosshard S, Pellet H, Piette JC, Sevestre H, Ducroix JP. Small-vessel vasculitis surrounding an uninflamed temporal artery: A new diagnostic criterion for polymyalgia rheumatica? Arthritis Rheum 2008;58:2565–2573. [PubMed: 18668584]
7. Seko Y, Minota S, Kawasaki A, Shinkai Y, Maeda K, Yagita H, Okumura K, Sato O, Takagi A, Tada Y. Perforin-secreting killer cell infiltration and expression of a 65-kD heat-shock protein in aortic tissue of patients with Takayasu's arteritis. J Clin Invest 1994;93:750–758. [PubMed: 7906697]
8. Brack A, Geisler A, Martinez-Taboada VM, Younge BR, Goronzy JJ, Weyand CM. Giant cell vasculitis is a T cell-dependent disease. Mol Med 1997;3:530–543. [PubMed: 9307981]
9. Weyand CM, Schonberger J, Oppitz U, Hunder NN, Hicok KC, Goronzy JJ. Distinct vascular lesions in giant cell arteritis share identical T cell clonotypes. J Exp Med 1994;179:951–960. [PubMed: 8113687]
10. Wagner AD, Goronzy JJ, Weyand CM. Functional profile of tissue-infiltrating and circulating CD68 + cells in giant cell arteritis. Evidence for two components of the disease. J Clin Invest 1994;94:1134–1140. [PubMed: 8083354]
11. Steinman RM, Banchereau J. Taking dendritic cells into medicine. Nature 2007;449:419–426. [PubMed: 17898760]
12. Pryshchep O, Ma-Krupa W, Younge BR, Goronzy JJ, Weyand CM. Vessel-specific Toll-like receptor profiles in human medium and large arteries. Circulation 2008;118:1276–1284. [PubMed: 18765390]
13. Krupa WM, Dewan M, Jeon MS, Kurtin PJ, Younge BR, Goronzy JJ, Weyand CM. Trapping of misdirected dendritic cells in the granulomatous lesions of giant cell arteritis. Am J Pathol 2002;161:1815–1823. [PubMed: 12414528]
14. Weyand CM, Ma-Krupa W, Pryshchep O, Groschel S, Bernardino R, Goronzy JJ. Vascular dendritic cells in giant cell arteritis. Ann N Y Acad Sci 2005;1062:195–208. [PubMed: 16461802]
15. Ma-Krupa W, Jeon MS, Spoerl S, Tedder TF, Goronzy JJ, Weyand CM. Activation of arterial wall dendritic cells and breakdown of self-tolerance in giant cell arteritis. J Exp Med 2004;199:173–183. [PubMed: 14734523]
16. Han JW, Shimada K, Ma-Krupa W, Johnson TL, Nerem RM, Goronzy JJ, Weyand CM. Vessel wall-embedded dendritic cells induce T-cell autoreactivity and initiate vascular inflammation. Circ Res 2008;102:546–553. [PubMed: 18202318]
17. Sanders CJ, Yu Y, Moore DA 3rd, Williams IR, Gewirtz AT. Humoral immune response to flagellin requires T cells and activation of innate immunity. J Immunol 2006;177:2810–2818. [PubMed: 16920916]
18. Niessner A, Sato K, Chaikof EL, Colmegna I, Goronzy JJ, Weyand CM. Pathogen-sensing plasmacytoid dendritic cells stimulate cytotoxic T-cell function in the atherosclerotic plaque through interferon-alpha. Circulation 2006;114:2482–2489. [PubMed: 17116765]
19. Yang X, Coriolan D, Murthy V, Schultz K, Golenbock DT, Beasley D. Proinflammatory phenotype of vascular smooth muscle cells: role of efficient Toll-like receptor 4 signaling. Am J Physiol Heart Circ Physiol 2005;289:H1069–H1076. [PubMed: 15863460]
20. Zeuke S, Ulmer AJ, Kusumoto S, Katus HA, Heine H. TLR4-mediated inflammatory activation of human coronary artery endothelial cells by LPS. Cardiovasc Res 2002;56:126–134. [PubMed: 12237173]
21. Schutyser E, Struyf S, Van Damme J. The CC chemokine CCL20 and its receptor CCR6. Cytokine Growth Factor Rev 2003;14:409–426. [PubMed: 12948524]
22. Williams IR. CCR6 and CCL20: partners in intestinal immunity and lymphorganogenesis. Ann N Y Acad Sci 2006;1072:52–61. [PubMed: 17057190]
23. Paradis TJ, Cole SH, Nelson RT, Gladue RP. Essential role of CCR6 in directing activated T cells to the skin during contact hypersensitivity. J Invest Dermatol 2008;128:628–633. [PubMed: 17882271]
24. Thomas SY, Banerji A, Medoff BD, Lilly CM, Luster AD. Multiple chemokine receptors, including CCR6 and CXCR3, regulate antigen-induced T cell homing to the human asthmatic airway. J Immunol 2007;179:1901–1912. [PubMed: 17641057]

25. Lim HW, Lee J, Hillsamer P, Kim CH. Human Th17 cells share major trafficking receptors with both polarized effector T cells and FOXP3+ regulatory T cells. J Immunol 2008;180:122–129. [PubMed: 18097011]

26. Weyand CM, Kaiser M, Yang H, Younge B, Goronzy JJ. Therapeutic effects of acetylsalicylic acid in giant cell arteritis. Arthritis Rheum 2002;46:457–466. [PubMed: 11840449]

27. Marcet B, Horckmans M, Libert F, Hassid S, Boeynaems JM, Communi D. Extracellular nucleotides regulate CCL20 release from human primary airway epithelial cells, monocytes and monocyte-derived dendritic cells. J Cell Physiol 2007;211:716–727. [PubMed: 17295217]

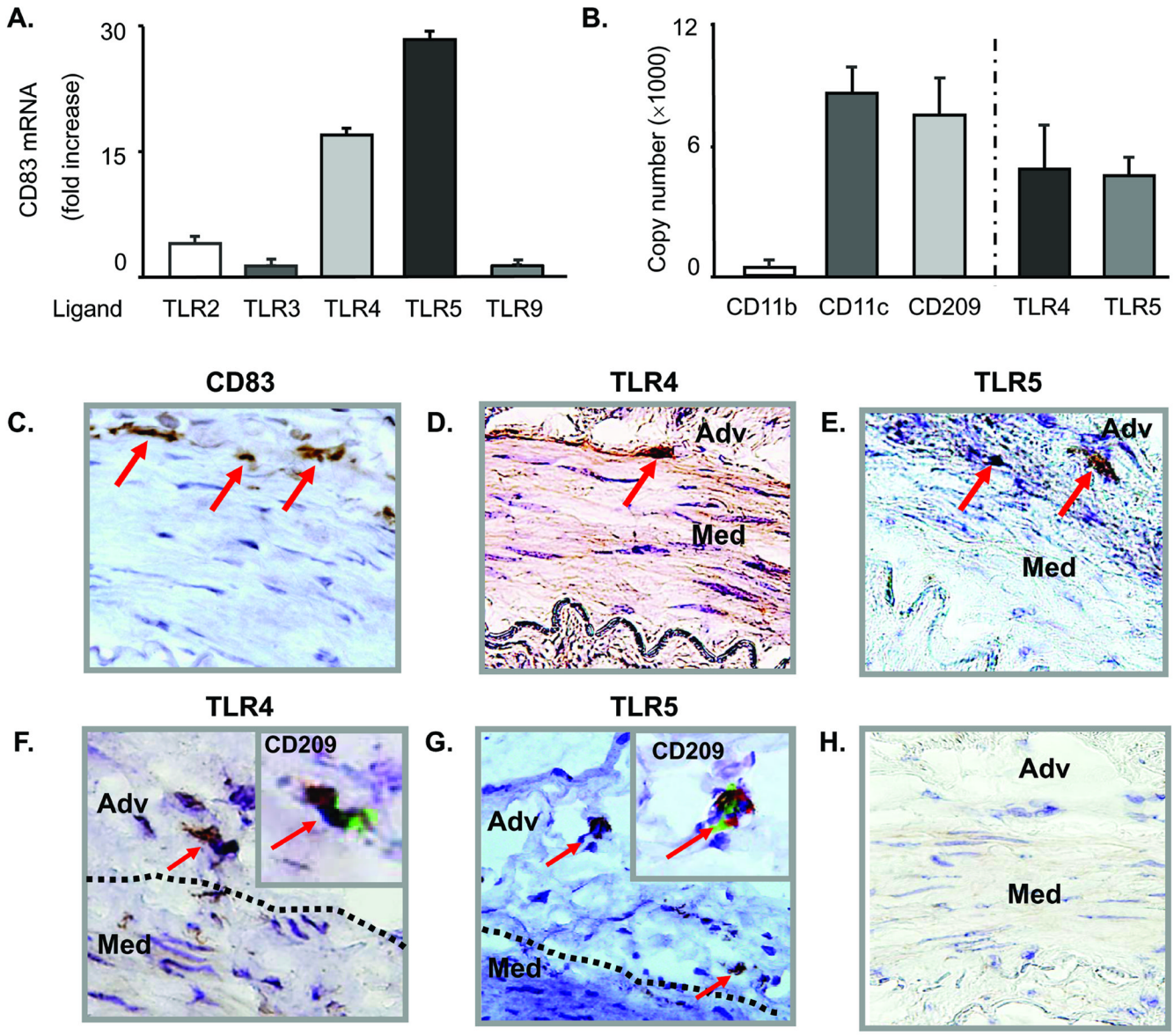

Figure 1. Specific activation of vascular DC by TLR4 and TLR5 ligands

Normal human temporal arteries were cultured in the presence of a panel of TLR ligands, and CD83 expression was analyzed by qPCR in tissue extracts. Results are expressed as fold induction compared to arteries cultured in the absence of any stimulator **(A)**. Expression of the macrophage marker CD11b and the DC markers CD11c and CD209 (DC-SIGN) were analyzed by qPCR in tissue extracts of normal human temporal arteries. Transcripts specific for TLR4 and TLR5 were abundant and present in comparable concentrations. Results are presented as mean ± SEM **(B)**. Induction of CD83 protein by TLR4 stimulation as detected by immunostaining **(C)**. Immunohistochemistry identified TLR4- **(D and F)** and TLR5-expressing DC **(E and G)** at the media-adventitia border. These cells expressed the DC marker CD209 as demonstrated by staining serial tissue sections **(inserts in F and G;** TLR protein brown, CD209 green**)**. Antibody isotype control **(H)**. Magnification × 400. Adv, adventitia; Med, media.

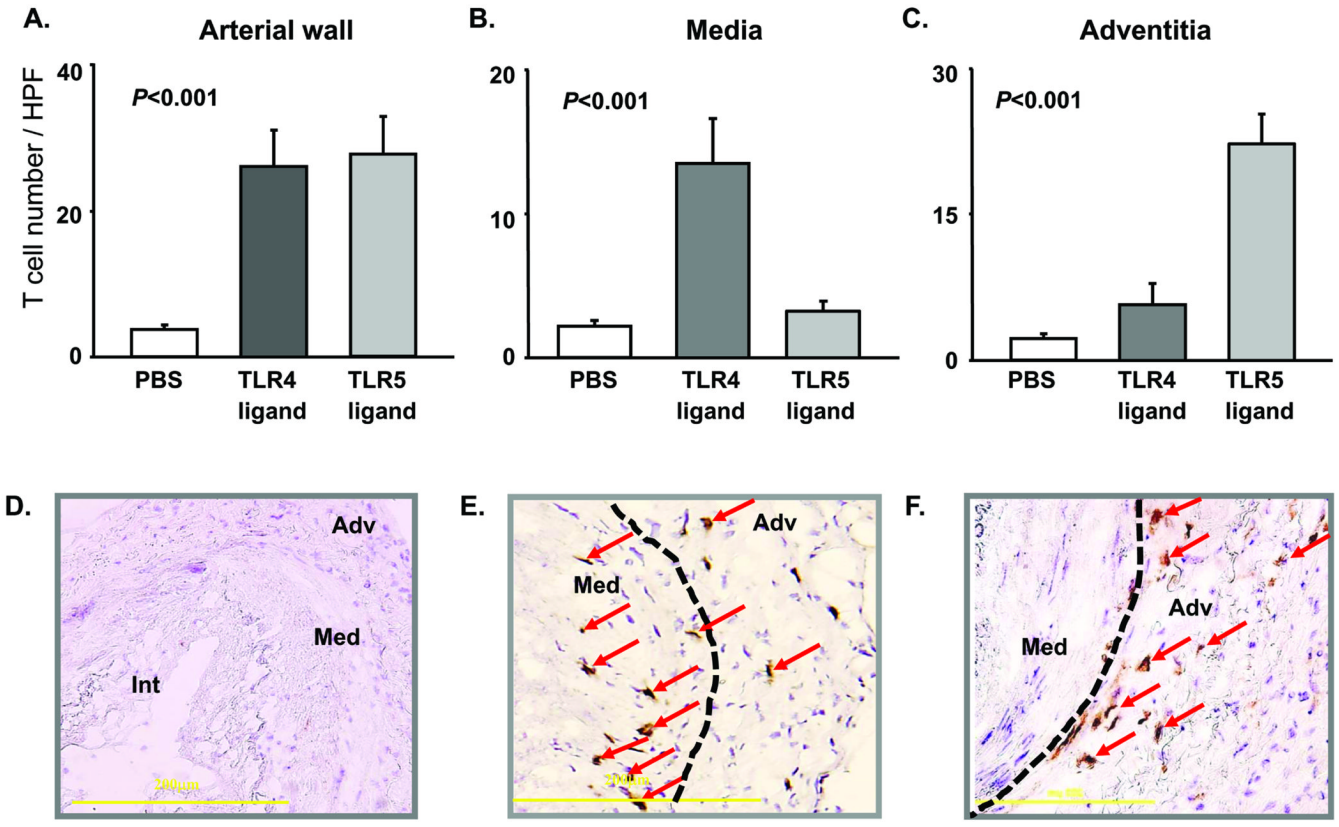

Figure 2. TLR4 and TLR5 stimulation initiates distinct types of vessel wall inflammation

Temporal arteries from 4 different donors were engrafted into SCID mice. On day 7, chimeras were treated with LPS (3μg/mouse) or flagellin (3μg/mouse), or sham injected with PBS. 24 h later, allogenic CD4 T cells were adoptively transferred by i.v. injection. One week later, artery grafts were harvested. Human T cells were identified by staining tissue sections with anti-CD3 antibodies (brown), and the density of T-cell infiltrates was assessed by counting T cells in the entire cross-section **(A)**, the media **(B),** and adventitia **(C)**. Results from 4 independent experiments are shown as mean ± SEM for arteries retrieved from PBS-injected **(D)**, LPS-treated **(E)**, and flagellin-treated **(F)** chimeras. CD3-positive cells (brown) are indicated by arrows; the media-adventitia border is marked by a dotted line. Original magnification ×200.

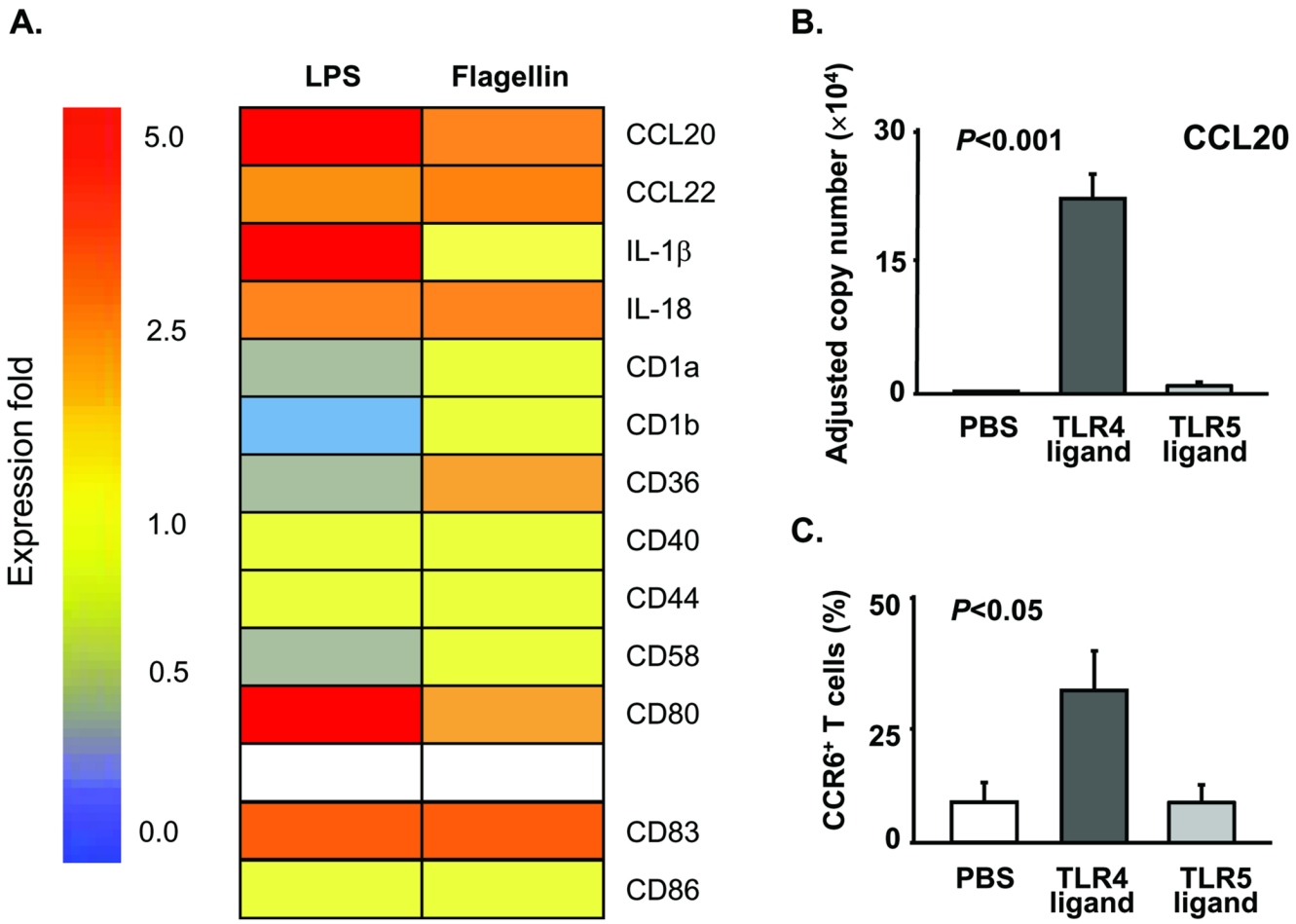

Figure 3. Differential induction of the T cell-attracting chemokine CCL20 in DC stimulated by TLR4 and TLR5 ligands

(**A**) DC generated from $CD14^+$ precursors were stimulated with LPS (1μg/ml), flagellin (1μg/ml), or PBS for 14 h. Total RNA was isolated, and gene expression was profiled with GEArrayTM Q and S Series Kits (SuperArray Bioscience Corporation, Frederick, MD). Expression levels for selected genes in LPS- or flagellin-stimulated DC as compared to control DC are presented as a heat-map pattern. **(B)** CCL20-specific transcripts were quantified by qPCR in DC treated with LPS, flagellin, or PBS. Mean ± SEM from 6 experiments. (**C**) Monocyte-derived DC triggered with PBS, LPS, or flagellin were tested for their T cell-attracting capacity in a transwell assay system. Purified CD4 T cells (10^5) were placed into the upper transwell inserts, and the insert was removed 2 h later. The number of $CCR6^+$ CD4 T cells in the lower chamber was analyzed by FACS with FITC-conjugated mouse anti-human CD4 and PE-conjugated mouse anti-human CCR6 antibodies. Mean ± SEM from 8 independent experiments.

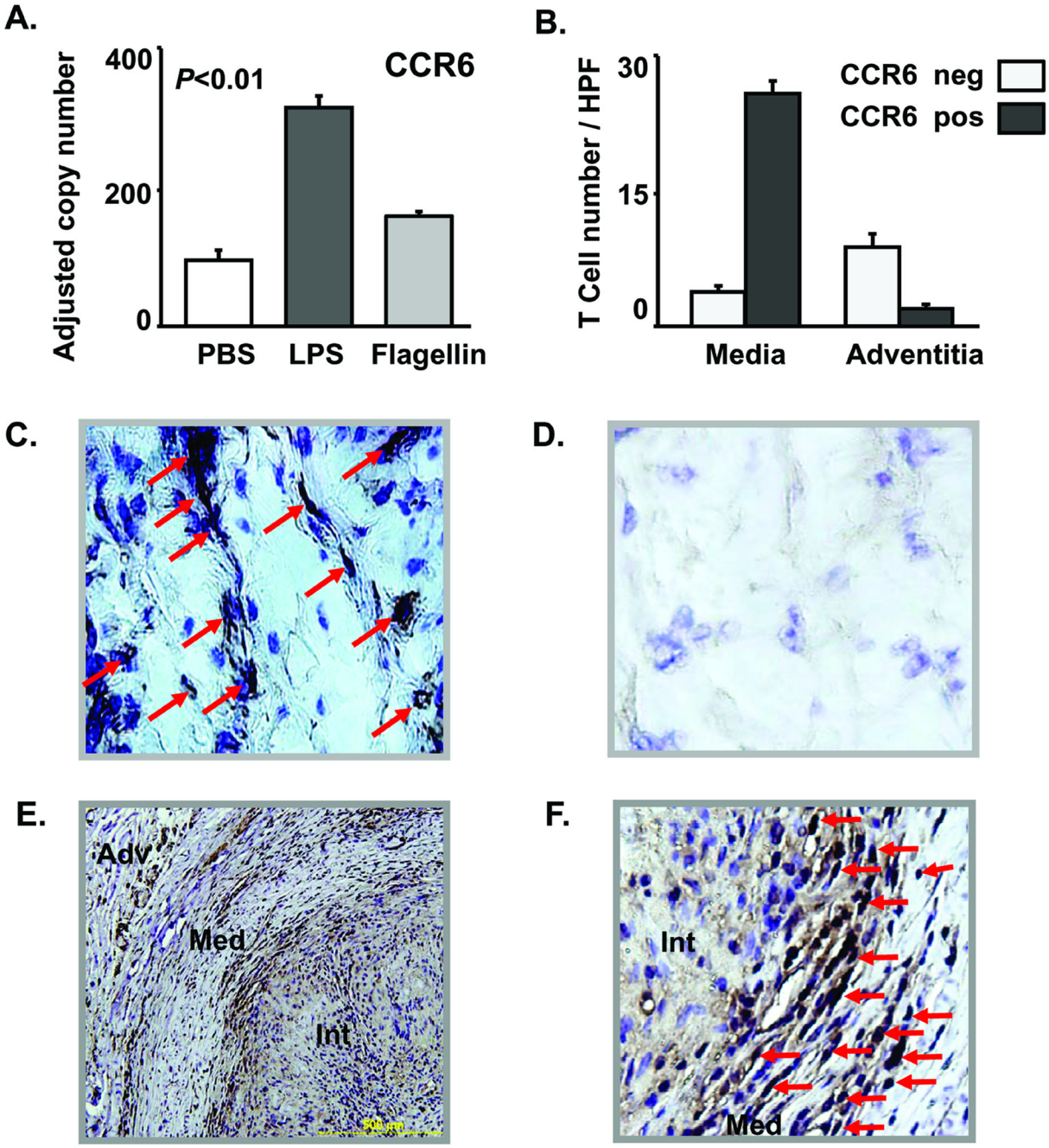

Figure 4. TLR4 stimulation induces transmural vascular inflammation by recruiting CCR6$^+$ CD4 T cells

Artery-SCID chimeras were treated with LPS (3μg/mouse), flagellin (3μg/mouse), or PBS on day 7 after engraftment. Human CD4 T cells (10^7 cells/mouse) were adoptively transferred on day 8. One week later, artery grafts were explanted. CCR6 **(A)** transcripts in the tissue were quantified by real-time PCR. Data are representative of 5 independent experiments and are shown as mean ± SEM. **(B, C)** Tissue sections from LPS-treated arteries were stained with anti-CCR6 antibodies or with isotype control antibodies. (**B**) CCR6$^+$ and CCR6$^-$ T cells were quantified in the medial and in the adventitial layer of LPS-pretreated grafts. (**C**) CCR6$^+$ T cells (marked with arrow) infiltrated into the smooth muscle cell layer. (**D**) Isotype control.

Cross-sections of temporal artery specimens with typical findings of GCA were stained with anti-CCR6 antibodies (**E, F**). $CCR6^+$ cells (brown stain) accumulate within the granulomatous infiltrates. **(F)** Abundant $CCR6^+$ mononuclear cells intermingle with multinucleated giant cells at the media-intima junction.

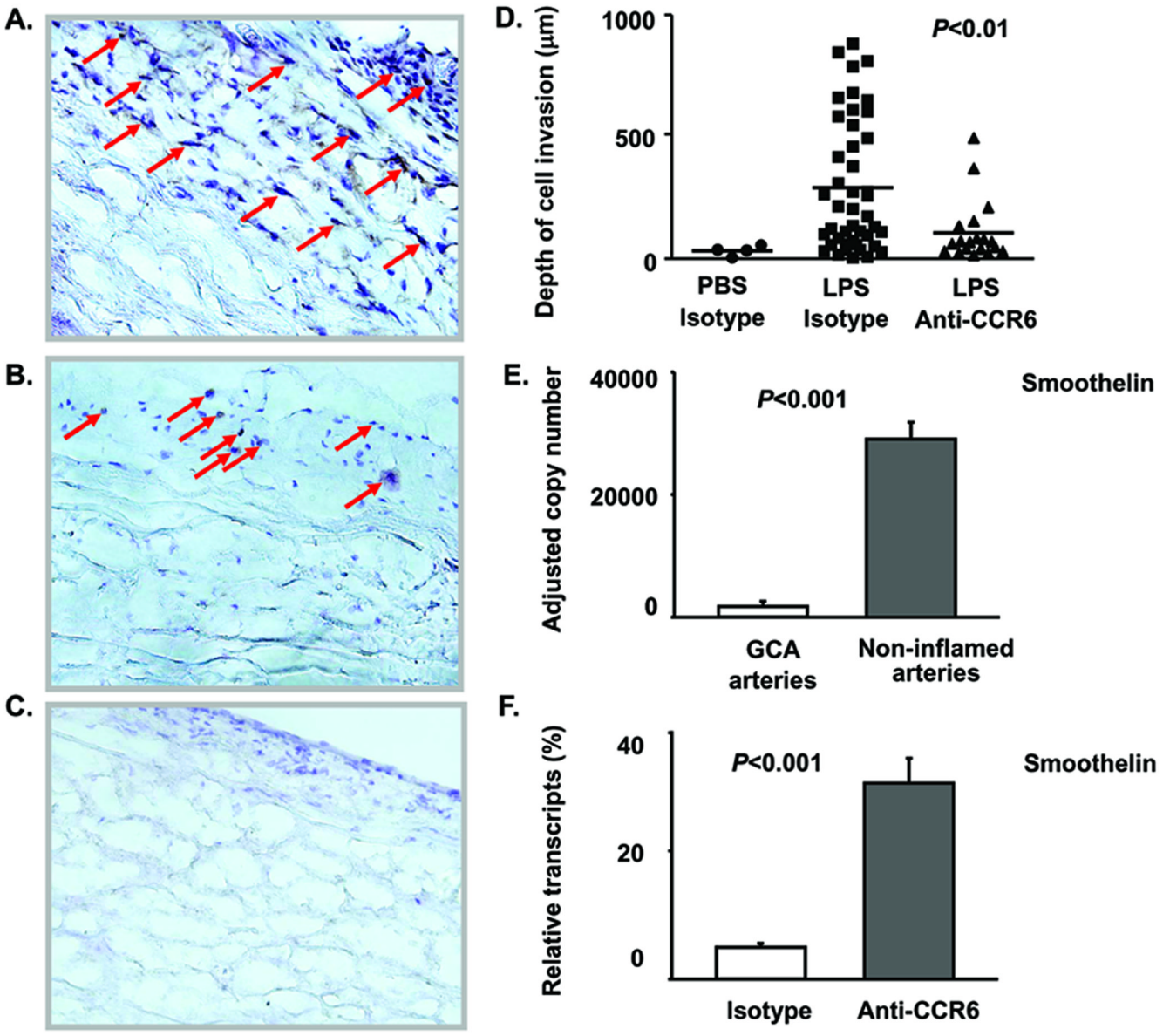

Figure 5. CCR6$^+$ T cells cause transmural vascular inflammation and smooth muscle cell injury

Temporal artery-SCID mouse chimeras were injected with LPS (3μg/ml) or PBS (control) on day 7 after implantation; 24 h later CD4 T cells combined with anti-CCR6 antibodies (50μg/ml) or isotype control antibody (50μg/ml) were adoptively transferred. One week later, grafts were harvested and human T cells (brown) were identified by immunohistochemistry for CD3. **(A)** Transmural T-cell infiltrates in grafts explanted from LPS-treated chimeras injected with CD4 T cells and isotype control antibody. **(B)** T cells in grafts from chimeras treated with LPS and adoptively transferred with CD4 T cells plus anti-CCR6 antibodies. **(C)** Minimal inflammatory infiltrates in arteries pretreated with PBS and adoptively transferred with CD4 T cells. (Original magnification × 200) **(D)** T-cell tissue invasion was quantified by measuring the distance of infiltrating T cells from the artery's surface using Image J1.36b software. Invasion distances for individual CD3 T cells were determined in 3 independent experiments. Mean invasion distances are indicated by bars. **(E, F)** VSMC injury was quantified by measuring transcripts of smoothelin, a gene product produced by healthy contractile VSMC.

(E) Smoothelin transcripts in GCA-affected (n=5) and non-inflamed control temporal arteries (n=5). Results are presented as mean ± SEM. (**F**) Recovery of smoothelin transcription by CCR6 blockade. Arteries were explanted from chimeras treated with LPS and adoptively transferred with CD4 T cells plus isotype control antibodies or anti-CCR6 antibodies. Smoothelin transcripts were quantified by qPCR and are expressed as percent of transcripts present in sham-treated arteries. Data represent 1 of 4 independent experiments and are given as mean ± SEM.

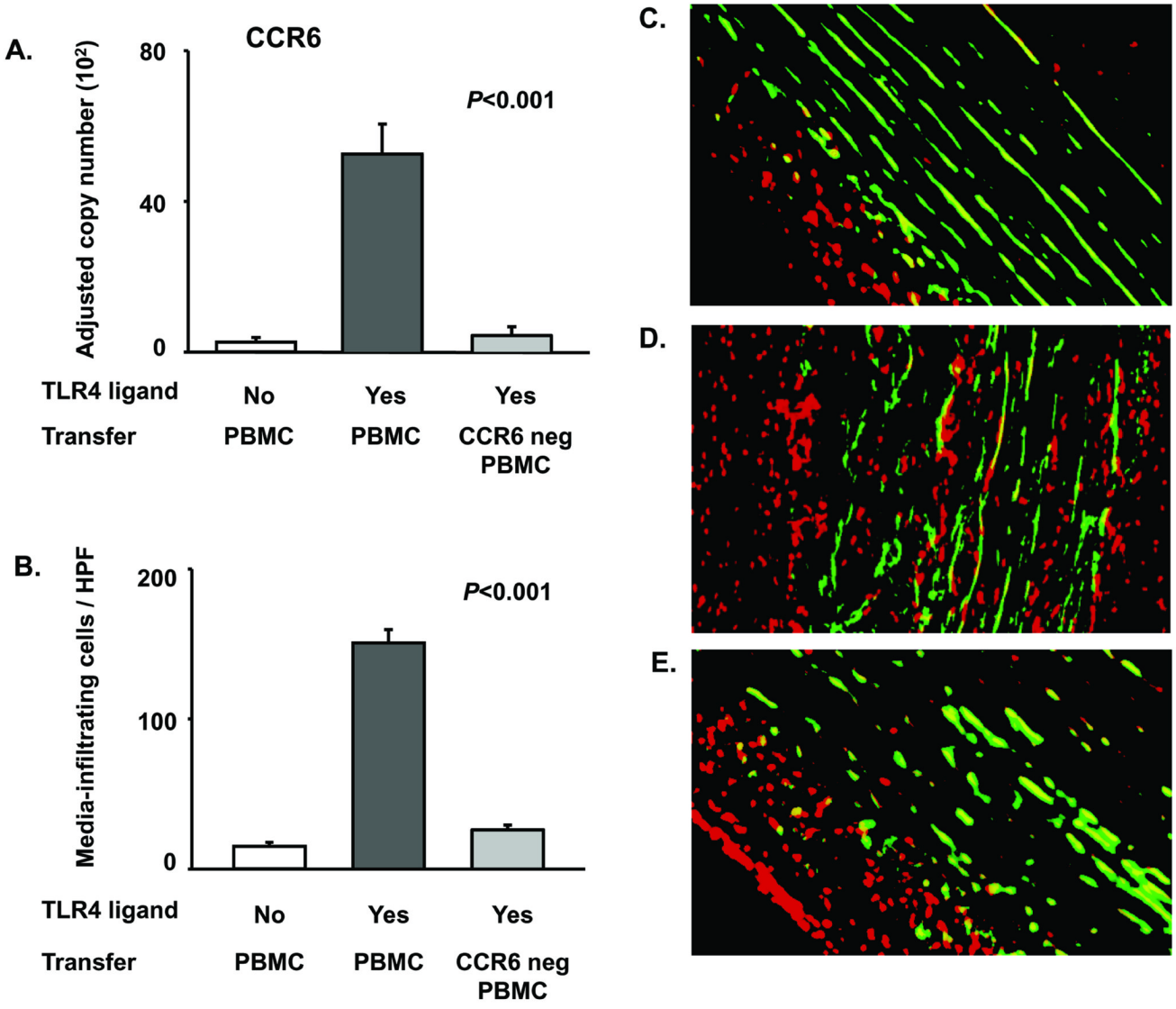

Figure 6. CCR6$^+$ T cells infiltrate into the vascular wall to cause panarteritis

Human artery-SCID chimeras engrafted with non-inflamed temporal arteries from 5 different donors were injected with LPS (3μg/ml) or PBS. Allogeneic PBMC (3×10^7 cells/mouse) which were un-separated or depleted of CCR6$^+$ cells were adoptively transferred. Arteries were explanted 1 week later. (**A**) CCR6 gene expression was quantified by real-time PCR. Results are presented as mean ± SEM. (**B–E**) Fluorescence microscopy for PI$^+$ cells to determine positioning of wall-infiltrating inflammatory cells. Media VSMC were identified through green autofluorescence. Numbers of PI$^+$ cells counted in a minimum of 10 high powered fields in each of 10 independent cross-sections are presented as mean ± SEM. (C, D, E) Positioning of tissue-infiltrating cells in arterial cross-sections. Green cells are VSMC; red cells are nuclei of infiltrating cells; nuclei of VSMC appear yellow due to the overlay of green and red. (C) Vascular infiltrate in the absence of TLR stimulation. (D) Vascular infiltrate generated by LPS pretreatment and adoptive transfer of un-separated PBMC. (E) Vascular infiltrate after LPS pretreatment and adoptive transfer of CCR6-depleted PBMC.